different Ni(001) unit meshes of the Ni(001)$c(2\times2)$O surface.

The main features of the potential plot in Fig. 4 are a central region of negative potential and regions of positive potential on the unit-mesh diagonals. These features are consonant with what is known about the structure of Ni(001)$c(2\times2)$O surface from LEED intensity analysis.[3] We attribute them to an adsorbed O atom located above the center of the square formed by four adjacent Ni atoms, and to diagonally directed Ni-O bonds, respectively.

Basically the reason that the lateral structure can be extracted directly from experiment is that our procedure in effect selects for observation a region where the potential is weak. In this region the lateral variations of potential cause interactions between two-dimensional free-electron states that are strong enough to measure by the improved technique described in this Letter, but at the same time weak enough to be treated theoretically as a small perturbation.

Some advantages of a method of surface-structure determination based on resonance dispersion measurements are apparent from the example described. The experiment itself is as simple as LEED and much simpler than angle-resolved UPS. With regard to interpretation, no large-scale computations are necessary as is the case for LEED intensity analysis; the lateral structure of the potential is obtained directly from experiment and does not involve computations for trial structures. The interpretation involves the dispersion of only one state and so is inherently simpler than in UPS where the dispersion of both an initial and a final state must be considered.

Helpful discussions with colleagues J. E. Rowe and M. A. Schluter are gratefully acknowledged.

[1]J. B. Pendry, *Low Energy Electron Diffraction* (Academic, New York, 1974).

[2]M. M. Traum, J. E. Rowe, and N. V. Smith, J. Vac. Sci. Technol. 12, 298 (1975).

[3]J. E. Demuth, D. W. Jepsen, and P. M. Marcus, Phys. Rev. Lett. 31, 540 (1973).

[4]K. Hirabayashi, J. Phys. Soc. Jpn. 25, 856 (1968).

[5]S. Miyake and K. Hayakawa, Acta Crystallogr., Sect. A 26, 601 (1970).

[6]E. G. McRae, Surf. Sci. 25, 491 (1971).

[7]E. G. McRae and C. W. Caldwell, Surf. Sci. 7, 41 (1967).

[8]V. Henrich, Surf. Sci. 49, 675 (1975).

[9]P. E. Best, Phys. Rev. Lett. 34, 674 (1975).

[10]E. G. McRae and C. W. Caldwell, Surf. Sci. 57, 63 (1976).

[11]A Hewlett-Packard 9830 calculator and associated interfacing to the experiment are used.

[12]L. R. Rabiner, J. H. McClellan, and T. W. Parks, Proc. IEEE 63, 595 (1975).

[13]J. H. McClellan, T. W. Parks, and L. R. Rabiner, IEEE Trans. Audio Electroacoust. 21, 506 (1973).

[14]Higher-energy bound states might be present but would not be observed in the present experiment because of its limited energy resolution (0.3 eV). Interactions involving the higher-energy states are probably very weak and are neglected here.

[15]The systematic differences near 15 and 23 eV are an experimental artifact that arises as explained previously (Refs. 4 and 7) from the use of a retarding field.

Spiral-Vortex Expansion Instability in Type-II Superconductors*

John R. Clem

Ames Laboratory–ERDA and Department of Physics, Iowa State University, Ames, Iowa 50011

(Received 28 February 1977)

It is shown that a flux vortex, in the presence of a sufficiently large current density applied parallel to its axis, is unstable against the growth of helical perturbations. This instability, which has an analog in magnetohydrodynamics, may play a critical role in current-carrying type-II superconductors subjected to longitudinal magnetic fields.

The behavior of spiral flux vortices in current-carrying type-II superconducting cylinders subjected to longitudinal magnetic fields is not yet completely understood. Still unresolved is the question of the vortex arrangement above the critical current, where a nonzero time-averaged longitudinal voltage and a longitudinal paramagnetic moment coexist. In this case, straightforward critical-state or force-balance calculations, modified to account for spiral vortices, yield a longitudinal moment but do not correctly predict the value of the critical current at which a voltage appears, nor are they capable of providing a satisfactory picture of a flux-flow state with a

nonzero longitudinal voltage.[1-5] Several authors[1,2] have suggested that fluxline cutting—the intersection and cross-joining of adjacent spiral vortices—might be the mechanism by which the critical state breaks down and a voltage appears. The conditions under which fluxline cutting occurs, however, are not as yet well known.

In this Letter, I show that a flux vortex, when subjected to a sufficiently large local current density applied parallel to its axis, is unstable to the growth of helical perturbations. I also show that this instability, which has an analog in magnetohydrodynamics, provides a specific mechanism for the triggering of fluxline-cutting events.

The forces exerted on a spiral vortex are best understood by first considering the Gibbs free energy as a function of the radius ρ of the imaginary cylinder on which the vortex axis lies. In the presence of a longitudinal applied magnetic field H_a and transport current I, where H_a and I are positive in the z direction, the Gibbs free energy $\Delta G'$ per unit length of a type-II superconducting cylinder of radius a containing a spiral vortex, relative to the energy in the Meissner state, can be written as the sum of three terms. One term, $\Delta G_s'$, arises from the self-energy of the vortex; the other two terms, $\Delta G_a'$ and Δ_T', describe the interaction between the vortex and the sources of H_a and I. The effective force per unit length of cylinder exerted on the vortex has only a radial component, $-d\Delta G'/d\rho$. Dividing this by the length of vortex per unit length of cylinder, one obtains the corresponding driving force (often referred to as the Lorentz force) per unit length of vortex $\vec{f}=\vec{f}_s+\vec{f}_a+\vec{f}_T=f_\rho\hat{\rho}$, where $\hat{\rho}$ is one of the usual unit vectors, $\hat{\rho}$, $\hat{\varphi}$, and $\hat{z}$ in cylindrical coordinates. Convenient approximate expressions for the three contributions to f_ρ are obtained as follows.

If the interaction of the vortex with its image in the cylinder wall is neglected, the self-energy per unit length of vortex is[6] $\varphi_0 H_{c1}/4\pi$, where $\varphi_0 = hc/2e$ is the flux quantum and H_{c1} is the lower critical field of the bulk superconductor. It is helpful to introduce the unit vector $\hat{\varphi}_0=\vec{\varphi}_0/\varphi_0 = \hat{\varphi}\sin\alpha+\hat{z}\cos\alpha$, defined as the local unit tangent to the vortex spiral in the sense of the vortex's self-field, where α is the pitch angle at radius ρ. If P denotes the pitch of the spiral, $\tan\alpha=\pm 2\pi\rho/P$, where the sign is positive (negative) for a right-handed (left-handed) spiral. The self-energy (or line-tension) contribution to the force, $\vec{f}_s = -(\varphi_0 H_{c1}/4\pi R_c)\hat{\rho}$, where $R_c=\rho/\sin^2\alpha$ is the radius of curvature of the spiral at radius ρ, describes the tendency of a spiral vortex to move to the center of the cylinder, where it has the shortest length and the least self-energy. This force also can be written as $\vec{f}_s=\vec{j}_{c1}\times\vec{\varphi}_0/c$, where $\vec{j}_{c1}=(c/4\pi)\nabla\times(H_{c1}\hat{\varphi}_0)$.

Using the London model[6] to calculate the interaction between the vortex spiral and the externally applied magnetic field and the current density, one obtains $\vec{f}_a=\vec{j}_a\times\vec{\varphi}_0/c$ and $\vec{f}_T=\vec{j}_T\times\vec{\varphi}_0/c$, where

$$\vec{j}_a=-\hat{\varphi}\left(\frac{cH_a}{4\pi\lambda}\right)\frac{I_1(\rho/\lambda)}{I_0(a/\lambda)}, \tag{1}$$

$$\vec{j}_T=\hat{z}\left(\frac{cH_T}{4\pi\lambda}\right)\frac{I_0(\rho/\lambda)}{I_1(a/\lambda)}, \tag{2}$$

$H_T=2I/ca$ is the current-induced self-field at the surface, and λ is the penetration depth. $\vec{j}_a$ and $\vec{j}_T$, the current densities produced in response to H_a and I, are obtained by solving Ampere's law and the first London equation[7] in cylindrical coordinates. $I_n(x)$ is the modified Bessel function of the first kind.

The net driving force per unit length of vortex is thus

$$f_\rho=-\frac{\varphi_0}{4\pi}\left[\frac{H_{c1}}{R_c}+\frac{H_a}{\lambda}\cos\alpha\frac{I_1(\rho/\lambda)}{I_0(a/\lambda)}+\frac{H_T}{\lambda}\sin\alpha\frac{I_0(\rho/\lambda)}{I_1(a/\lambda)}\right]. \tag{3}$$

Consider the fate of a right-handed spiral vortex nucleated at the surface with its axis locally aligned along the net magnetic field at the surface, $H_T\hat{\varphi}+H_a\hat{z}$ ($H_T>0$ and $H_a>0$). The pitch angle at nucleation is $\alpha_{en}=\tan^{-1}(H_T/H_a)$, the pitch is $P_{en}=2\pi a(H_a/H_T)$, and the radius of curvature is $R_c(a)=a(1+H_a^2/H_T^2)$. The force on the vortex is seen from Eq. (3) to be radially inward, since all terms within the brackets are positive. The vortex spiral thus maintains a constant pitch as it contracts around the cylinder axis. The terminal velocity $\vec{v}$ of the contracting vortex can be approximated by balancing the driving force $\vec{f}$ and the viscous drag force $-\eta\vec{v}$, where η is a phenomenological viscous drag coefficient[8] per unit length of vortex.

When the vortex spiral reaches the cylinder axis, f_ρ vanishes, since the radius of curvature is infinite and both ρ and the pitch angle vanish there. One is tempted to assume that the cylinder axis represents a stable final resting place for a

straight vortex. This assumption is not always correct, however, for such a vortex is susceptible to the growth of a helical perturbation if the applied current is sufficiently large. For the situation just considered, although a right-handed spiral fluctuation is damped, a deformation of the vortex into a left-handed spiral with pitch P and wave number $k = 2\pi/P$ can grow, as can be seen by writing the corresponding driving force per unit of vortex as $f_\rho = K(\rho, k)\rho$, where

$$K(\rho, k) = (\varphi_0/4\pi\lambda^2)[1 + (k\rho)^2]^{-1/2}[H_T a_1 k\lambda I_0(\rho/\lambda) - H_{c1}(k\lambda)^2[1 + (k\rho)^2]^{-1/2} - H_a a_0 I_1(\rho/\lambda)(\tfrac{1}{2}\rho/\lambda)^{-1}], \quad (4)$$

$a_1 = [I_1(a/\lambda)]^{-1}$, and $a_0 = [2I_0(a/\lambda)]^{-1}$. For fixed values of H_T, H_{c1}, and H_a, $K(0, k)$ has its maximum value,

$$K_{\max}(0) = (\varphi_0 a_1^2/16\pi\lambda^2 H_{c1})(H_T^2 - H_{Tc}^2), \quad (5)$$

for $k = k_{\max} = a_1 H_T/2\lambda H_{c1}$, where

$$H_{Tc} = (2a_0^{1/2}/a_1)(H_a H_{c1})^{1/2}. \quad (6)$$

If $H_T > H_{Tc}$, $K(0, k) > 0$ for all values of k in the range $k_- < k < k_+$, where

$$k_\pm = \lambda^{-1}(a_1/2H_{c1})[H_T \pm (H_T^2 - H_{Tc}^2)^{1/2}]. \quad (7)$$

Thus, for fixed H_{c1} and H_a, if $H_T > H_{Tc}$, any left-handed spiral fluctuation with k in the above range is unstable. The initial growth rate of the instability, obtained by balancing the driving force and the viscous drag force, is $\beta = \rho^{-1}d\rho/dt = K(0, k)/\eta$. The mode of maximum instability has $k = k_{\max}$. It also can be shown that if $K(\rho, k)$ is positive for an infinitesimal fluctuation with $\rho \approx 0$, it remains positive for all ρ out to the specimen radius a.

The above-described spiral-vortex expansion instability has a close analogy with a magnetohydrodynamic instability, called the spiral, helical, or cork-screw instability, in which a cylindrical column of conducting fluid carrying a current in a longitudinal magnetic field is subject to the growth of spiral distortions of the column.[9-12] The destabilizing influence has been shown[9-14] to be the Lorentz force density $\vec{J}\times\vec{B}/c$ exerted by the applied magnetic flux density $\vec{B}$ upon the current density $\vec{J}$, which is parallel to the spiraling axis of the fluid column. The spiral-vortex expansion instability is the analog of this instability, except that the roles of the magnetic flux density and the electrical current density are interchanged. Here the destabilizing influence is the driving force per unit length $\vec{j}_T\times\vec{\varphi}_0/c$ exerted by the applied current density $\vec{j}_T$ upon the quantum of flux $\vec{\varphi}_0$, which is parallel to the spiraling axis of the vortex.

A positive time-averaged longitudinal voltage can be generated along a superconducting cylinder by the following periodic sequence of motions of a single spiral vortex, provided the spiral expansion instability is at work. As the cycle begins, the cylinder contains no vortices. If the values of H_a and $H_T = 2I/ca$ ($H_a > 0$ and $H_T > 0$) are such that one vortex, but no more than one, is produced in the cylinder, then a right-handed vortex spiral of pitch $P_{en} = 2\pi a(H_a/H_T)$ is nucleated. The vortex then moves to the cylinder axis, where, for sufficiently large H_T, it becomes susceptible to the spiral-vortex expansion instability. An unstable left-handed spiral, whose most probable pitch is $P_L = 2\pi/k_{\max}$, grows and expands outward until it annihilates at the surface, restoring the cylinder to its initial condition and preparing it for the beginning of another cycle. If the frequency of this cyclic motion is ν, the time-averaged electric field along the length of the cylinder is $\bar{E}_z = (h\nu/2e)(P_{en}^{-1} + P_L^{-1})$. Since each spiral flux vortex contributes to the longitudinal flux while it is in the cylinder, the succession of spiral vortices makes a positive contribution to the time-averaged longitudinal flux. However, since each flux quantum that enters the cylinder later exits again in a kind of breathing motion, the time-averaged longitudinal flux does not increase with time.

When more than one vortex is present in the cylinder, a positive time-averaged longitudinal voltage can be generated by a more complex periodic sequence of motions of spiral vortices, again provided the spiral-vortex expansion instability can occur. The simplest example of this is sketched in Fig. 1. As the cycle begins [Fig. 1(a)], a straight vortex initially resides along the axis of the cylinder, but the combination of H_a and H_T is not quite sufficient to make this vortex unstable. If the values of H_a and H_T are such that no more than two vortices are in the cylinder at one time, a second right-handed spiral vortex of pitch $P_{en} = 2\pi a(H_a/H_T)$ is nucleated at the surface. As the spiral contracts, the additional current density generated by this vortex along the cylinder axis causes the first vortex to undergo a spiral instability and to deform into a left-hand-

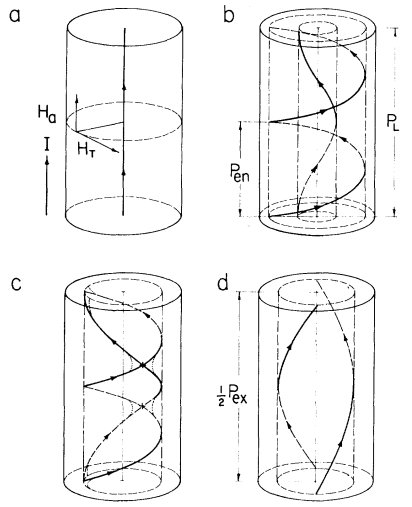

FIG. 1. Cyclic motion of two vortices, producing a longitudinal voltage. (a) First vortex lies along cylinder axis. Applied magnetic field H_a and current-induced self-field $H_T = 2I/ca$ causes nucleation of a second right-handed spiral vortex of pitch P_{en}. (b) First vortex undergoes spiral-vortex expansion instability and deforms into left-handed spiral of pitch P_L. (c) Spirals intersect and cross-join (dotted lines). (d) Resulting double helix of pitch P_{ex} is unstable. One spiral contracts to the center and the other exits.

ed spiral of pitch P_L, which expands outward to meet the contracting spiral [Fig. 1(b)]. The two spirals intersect, cross-join [Fig. 1(c)], and then straighten into two spirals (a double helix) of the same pitch P_{ex}, where $P_{ex}^{-1} = \frac{1}{2}|P_{en}^{-1} - P_L^{-1}|$ [Fig. 1(d)]. Since the two resulting spirals repel each other with a greater force than did the original vortices, one spiral contracts around the cylinder axis and simultaneously repels the other one outward unitl it annihilates at the surface, restoring the cylinder to its initial condition. If the frequency of this cyclic motion is ν and if the existing vortices are right-handed spirals (of pitch $P_{ex} > P_{en}$), the time-averaged electric field along the length of the cylinder is $\bar{E}_z = (h\nu/2e)(P_{en}^{-1} - P_{ex}^{-1})$.

Extension of the above analysis to a large number of vortices leads to the following detailed picture of how a nonzero time-averaged longitudinal voltage and a time-averaged paramagnetic moment can coexist in a type-II superconducting cylinder carrying a current in an applied longitudinal magnetic field: Spiral vortices periodically nucleate at the surface, and as they contract inward, they cause the spiral-vortex expansion instability to occur throughout the interior of the cylinder. Fluxline-cutting events that are triggered by the spiral instability at the center produce pitch lengthening of vortex spirals next to the cylinder axis. Additional fluxline-cutting events, triggered by the spiral instability throughout the remainder of the cylinder cross section, pass this pitch lengthening from the center toward the surface. When the outermost, last-nucleated spiral vortices of pitch P_{en} undergo fluxline cutting, they are transformed into an equal number of spiral vortices of increased pitch P_{ex}. These new vortices are repelled outward, such that they annihilate at the cylinder surface. Although there is thus no net increase in the number of longitudinal flux quanta over a cycle, a nonzero longitudinal electric field $\bar{E}_z$ nevertheless is generated because the pitch of the entering spiral vortices is less than that of the exiting ones. If ν is the rate at which spiral vortices nucleate, $\bar{E}_z = (h\nu/2e)(P_{en}^{-1} - P_{ex}^{-1})$. The paramagnetic moment can be understood in terms of a more familiar critical-state or force-balance theory,[1,2,5,15] in which spiral vortices adopt a force-free or nearly force-free configuration of currents and fields.

*Work performed for the U. S. Energy Research and Development Administration under Contract No. W-7405-eng-82.

[1]A. M. Campbell and J. E. Evetts, *Critical Currents in Superconductors* (Taylor and Francis, London, 1972), p. 61.

[2]W. E. Timms and D. G. Walmsley, J. Phys. F 5, 287 (1975).

[3]J. R. Clem, Phys. Lett. 54A, 452 (1975).

[4]W. E. Timms and D. G. Walmsley, J. Phys. F 6, 2107 (1976).

[5]R. Gauthier, Ph.D. thesis, University of Ottawa, Canada, 1976 (unpublished).

[6]A. L. Fetter and P. C. Hohenberg, in *Superconductivity*, edited by R. D. Parks (Marcel Dekker, New York, 1969), Vol. 2, p. 817.

[7]F. London, Superfluids, Macrospic Theory of Superconductivity (Dover, New York, 1961), Vol. 1, p. 29.

[8]Y. B. Kim and M. J. Stephen, in *Superconductivity*, edited by R. D. Parks (Marcel Dekker, New York, 1969), Vol. 2, p. 1107.

[9]A. Dattner, B. Lehnert, and S. Lundquist, in Proceedings of the Second U. N. Conference on the Peaceful Uses of Atomic Energy, Geneva, Switzerland (Pergamon, Oxford, 1958), Vol. 31, p. 325.

[10]A. Dattner, Ark. Fys. 21, 71 (1962).

[11]U. Ingard and D. Wiley, Phys. Fluids 5, 1500 (1962).

[12]M. N. Yuen, Phys. Fluids 9, 1140 (1966).

[13]R. J. Tayler, Rev. Mod. Phys. 32, 907 (1960).

[14]G. Murty, Ark. Fys. 19, 483 (1961).

[15]J. R. Clem, to be published.